

Article

Down to the Crust: Chemical and Mineralogical Analysis of Ceramic Surface Encrustations on Bronze Age Ceramics from Békés 103, Eastern Hungary

Mark Golitko ^{1,*}, Alyssa McGrath ¹, Attila Kreiter ², Ian V. Lightcap ³ , Paul R. Duffy ⁴, Györgyi M. Parditka ⁵ and Julia I. Giblin ⁶

¹ Department of Anthropology, University of Notre Dame, Notre Dame, IN 46556, USA; amcgrat3@nd.edu

² Hungarian National Museum, 1088 Budapest, Hungary; attila.kreiter@gmail.com

³ Center for Sustainable Energy, University of Notre Dame, Notre Dame, IN 46556, USA; ilightca@nd.edu

⁴ The Archaeology Centre, University of Toronto, Toronto, ON M5S 2S2, Canada; paul.duffy@utoronto.ca

⁵ Department of Anthropology, University of Michigan, Ann Arbor, MI 48109, USA; gypardit@umich.edu

⁶ Department of Sociology, Criminal Justice, and Anthropology, Quinnipiac University, Hamden, CT 06518, USA; Julia.Giblin@quinnipiac.edu

* Correspondence: mgolitko@nd.edu



Citation: Golitko, M.; McGrath, A.; Kreiter, A.; Lightcap, I.V.; Duffy, P.R.; Parditka, G.M.; Giblin, J.I. Down to the Crust: Chemical and Mineralogical Analysis of Ceramic Surface Encrustations on Bronze Age Ceramics from Békés 103, Eastern Hungary. *Minerals* **2021**, *11*, 436. <https://doi.org/10.3390/min11040436>

Academic Editor: Adrián Durán Benito

Received: 2 April 2021

Accepted: 16 April 2021

Published: 20 April 2021

Publisher's Note: MDPI stays neutral with regard to jurisdictional claims in published maps and institutional affiliations.



Copyright: © 2021 by the authors. Licensee MDPI, Basel, Switzerland. This article is an open access article distributed under the terms and conditions of the Creative Commons Attribution (CC BY) license (<https://creativecommons.org/licenses/by/4.0/>).

Abstract: Békés 103, a primarily Middle Bronze Age (c. 1600–1280 calBC) cemetery and settlement on the Great Hungarian Plain, has been investigated by the BAKOTA project since 2011. Ceramics from the site are covered in dense white concretions, and it has been noted during compositional analyses that these vessels exhibit elevated concentrations of several potentially mobile elements in comparison to vessels from regional tell sites. Here, we use a multimethod (optical mineralogy, FT-IR, XRD, XPS, PXRF, SEM-EDS, and LA-ICP-MS) mineralogical and chemical approach to characterize the composition of surface encrustations on ceramics samples from Békés 103. We also chemically map interior paste composition using LA-ICP-MS to identify potential leaching of mobile elements into or out of vessel bodies. We demonstrate that the surface encrustations are primarily composed of calcite but also contain a variety of other mineral and organic constituents indicative of deposition of soil carbonates, phosphates, nitrates, and other inorganic and organic components. We further document the leaching of several mobile elements into ceramic pastes as well as formation of secondary calcite along void, pore, and temper boundaries. The presence of cremated bone and possibly bone ash in close vicinity to many of the studied vessels may also have contributed to the observed patterns of diagenesis. It is likely that similar post-burial processes might affect ceramics from other sites located in low-lying, seasonally inundated contexts.

Keywords: Great Hungarian Plain; Bronze Age; encrustation; calcite; ceramic diagenesis

1. Introduction

It is well understood that the composition of archaeological ceramics may reflect a variety of geological, cultural, and environmental factors that together generate the final mineralogical and chemical composition as observed by the archaeologist [1]. These factors encompass local geology and choices of clay selection, mixing, and temper addition, but also what happens after a ceramic object has entered the burial environment. In the present study, we investigate the composition of surface encrustations on ceramics from the Bronze Age (primarily 1600–1280 calBC) urn cremation cemetery of Békés 103 “Jégvermiker” to determine the origin of this material and what impact it might have on internal sherd chemistry. This study is part of the broader BAKOTA (Bronze Age Körös Off Tell Archaeology) project, which examines how this large cemetery integrates into the broader social world of the Bronze Age Carpathian Basin [2,3].

Most of the ceramics recovered at Békés 103 are coated in a thick layer of whitish-grey material that covers the original reduced and burnished ceramic surface. While Bronze

Age vessels in nearby Transdanubia in some cases had deliberate surface applications (so-called “Encrusted Ware”), the surface encrustations at Békés 103 are clearly non-cultural, as they cover both original vessel surfaces and ancient breaks. In the present study, we employ mineralogical and chemical methods to determine the chemical and mineralogical composition of these surface encrustations, as well as mapping the internal distribution of potentially mobile elements within the ceramic paste to examine the impact of elemental uptake from the burial environment. The primary goal of this study is to understand to what degree the measured chemistry of sherds from Békés 103 might be representative of their original production composition as a preliminary step in attempting to compositionally provenience vessels from the site. Our analysis suggests that a suite of mobile elements has also variably altered the original paste composition of ceramics at the site, impacting the results of any potential future compositional analyses of ceramics from Békés 103 and other flat sites on the Great Hungarian Plain (GHP), which are likely impacted by similar soil chemistry and high moisture levels.

The Békés 103 “Jégvermi-Kert” Cemetery Ceramic Assemblage

Békés 103 “Jégvermi-kert” is a large cemetery and associated settlement located along a meander of the Kettős-Körös River in Békés County, eastern Hungary (Figure 2). The site was first identified during the 1990s as part of national *Magyarország Régészeti Topográfiaja* (MRT) surveys of the region, and has been extensively excavated by the BAKOTA project since 2011 [2,4]. Early work at the site focused on mapping and small excavations of the settlement portion of the site, but for much of the decade, work has focused on the associated cemetery [5]. To date, 84 graves have been excavated; however, it is estimated that there may be as many as 2600 or more total burials at the site [4]. While there are a handful of inhumation burials present, the majority are cremation burials, which typically consist of a large burial urn containing the cremated remains of one or more individuals, usually covered with a bowl or platter as a lid. These urns are typically accompanied by a small handled cup (see Figure 1A), or in rarer cases by multiple cups or smaller bowls and urns [2,4–6].

Available radiometric dates suggest initial use of the cemetery during the Early Bronze Age (EBA) beginning around 2460 calBC, with the latest burials dating to the Late Bronze Age (LBA, final usage c. 1010 calBC). However, on present evidence the primary usage of the cemetery appears to date to the Middle Bronze Age (MBA), between approximately 1600 and 1280 calBC [2]. Demographic modelling suggests that the cemetery may have been larger than the size of its associated settlement could account for, and individuals from a broader region around the site may have been interred there, a pattern similar to that further south along the Maros River during the MBA [4,7]. From 2013 onwards, a program of mineralogical and chemical study of ceramics was carried out in conjunction with analyses of MBA pottery from several regional tell sites (Figure 2) to examine whether burial ceramics at Békés 103 were derived from a broader region of the eastern GHP or were primarily locally produced [8]. To date, sherds from 98 vessels at Békés 103 have been chemically characterized by LA-ICP-MS. As part of this study, over 100 clay samples were collected from locations east of the Tisza River as well as in the area around modern Budapest (Figure 2) to establish a geochemical baseline for the region.

When excavated, the majority of the ceramics from Békés 103 were covered in a whitish-grey crust (Figure 1). During ceramic reconstruction and analysis, this crust is typically manually removed with a scalpel to reveal the burnished reduced vessel surfaces and channeled decorations characteristic of the Bronze Age ceramics of the region. While surface encrustations are not generally associated with the Otomani–Gyulavarsánd style area to which the MBA component at the Békés 103 cemetery belongs, encrustation as a deliberate decorative technique was already present on the GHP during the early Copper Age (Tiszapolgár Culture, c. 4500–3800 cal BC) [9]. By the time of the MBA phases at Békés 103, pottery-surface encrustation was a relatively common practice in many parts of Europe, including on contemporary Beaker pottery [10,11] and as a defining characteristic of the

Transdanubian Encrusted Pottery Culture, c. 2200/2000–1500/1400 BC [11–16]. Encrustations on these vessels were typically produced using burnt bone (presumed mammalian) and bonded into incised decorations with an organic binder such as mastic [9,14]. General commonalities of burial practices in the broader region of the GHP and Transdanubia during the MBA [17], as well as sharing of many common motifs and even vessel forms [18,19], allow for the possibility that the encrustations on ceramics from Békés 103 could be a deliberate practice borrowed from communities farther to the west. It is, however, clear that the encrustations are not anthropogenic and likely result from post-depositional processes. Encrustation appears on both inner and outer vessel surfaces, and more importantly, clearly covers over ancient breaks on some sherds (see Figure 3A).

It is not clear, however, what the composition of this material is and what constituents of the burial environment (or original internal sherd composition) specifically contributed to its formation. Visually, the crust varies between off-white to light grey (Figure 1B), with variable thickness ranging up to an observed maximum of 1.5 mm. Under magnification, opaque mineral grains (including hematite), mica flakes (which are abundant in surrounding sediments), and small root fragments are visible within or adhering to the encrustation. Viewed in cross-section (Figure 1B–F), it is evident that the crust is inhomogeneous and exhibits distinctive layers or regions of variable texture, including voids lined with feathery calcite crystals.

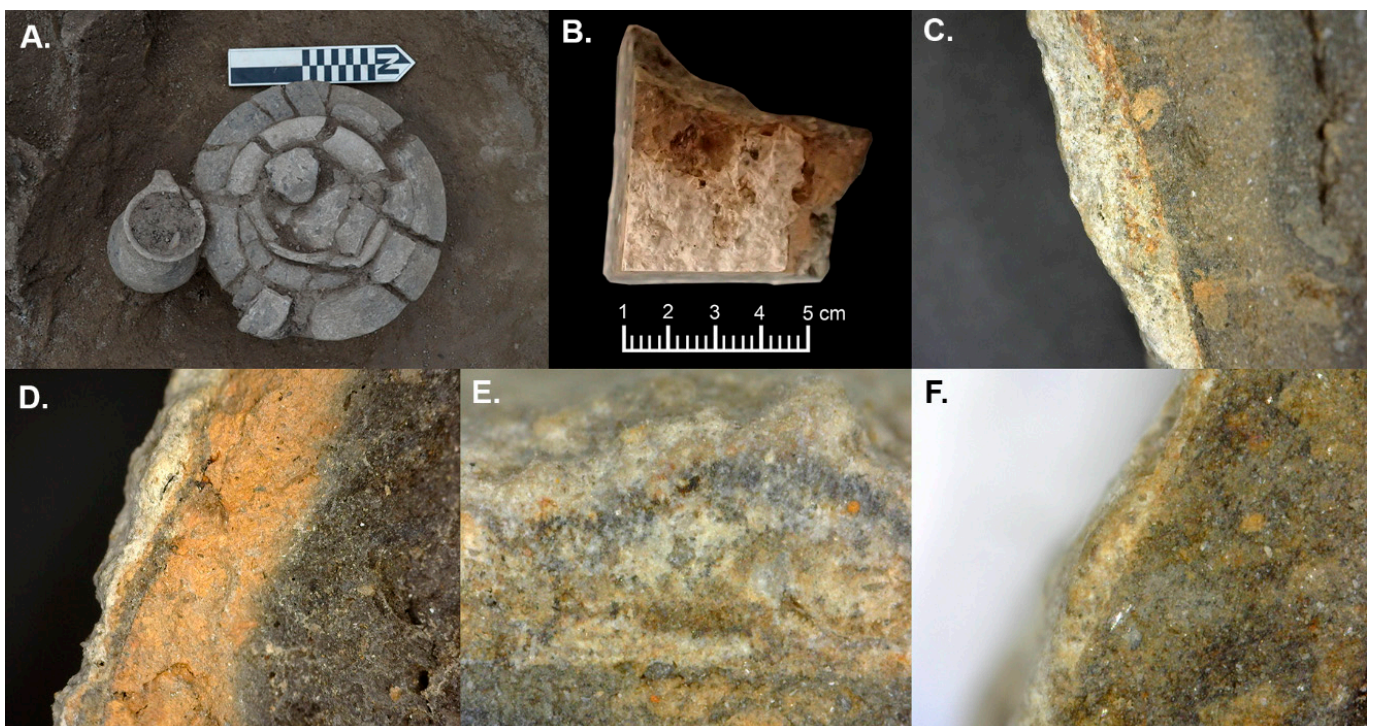


Figure 1. (A) Burial HB27 (3107 ± 24 bp/ 1400 ± 32 calBC) during excavation showing a typical cremation burial at Békés 103. (B) Outer surface of sherd ID005 (right) showing whitish encrustation. (C) ID005 cross-section ($50\times$ magnification) showing the boundary between the vessel paste and encrustation. (D) Sherd SS1071 cross-section ($50\times$ magnification) showing the interface between the crust and reduced burnished vessel surface. (E) Encrustation-sherd boundary on ID005 ($200\times$ magnification) highlighting the layering and texture present within the surface encrustation. (F) Sherd-encrustation boundary on sample ID009 ($200\times$ magnification) showing region of relatively thin crust.

The most probable source of the encrusted material is deposition of dissolved carbonates and phosphates from the surrounding soil matrix [20]. Békés 103 is a flat (non-tell) site located along a former meander of the Kettős-Körös River, and even today is prone to flooding during periods of high rainfall. However, prior to extensive 19th century drainage and canalization, much of the Békés area consisted of seasonally inundated swamps, and

the ceramics there have likely undergone several thousand years of repeated seasonal soaking and drying [21]. Similar encrustations are also present on ceramics from the nearby roughly contemporaneous settlement site of Tarhos 26 [22], suggesting that this issue may be more general to flat sites in lower-lying areas of the GHP.

Chemical and mineralogical analysis suggests that almost all of the ceramics excavated at Békés 103 were made from loess-derived clays local to the GHP. Pastes contain quartz, muscovite mica, feldspar, and occasional clay pellets, and show little evidence of significant clay processing beyond the occasional addition of grog temper. When compared to ceramics analyzed from the four other regional sites, all of which are elevated tell settlements (see Figure 2), it was noted that the ceramics from Békés 103 have elevated concentrations of a number of potentially mobile elements, including Ca, P, Sr, and Ba. These elements are particularly prone to mobilization in groundwater and can be readily incorporated into ceramic paste [23–29], particularly in lower-fired ceramics that retain significant cation exchange capacity [30]. Analyses of ceramics from Békés 103 and other EBA and MBA sites from the GHP and Transdanubia suggest that Bronze Age firing rarely reached temperatures above 700 °C (based on the presence of unaltered calcareous inclusions in some sherds and optical activity of groundmass in thin-section) [31–34]. This suggests that the ceramics from Békés 103 should retain a relatively high cation exchange capacity, while lacking high temperature mineral phases that are susceptible to decomposition [26,35].

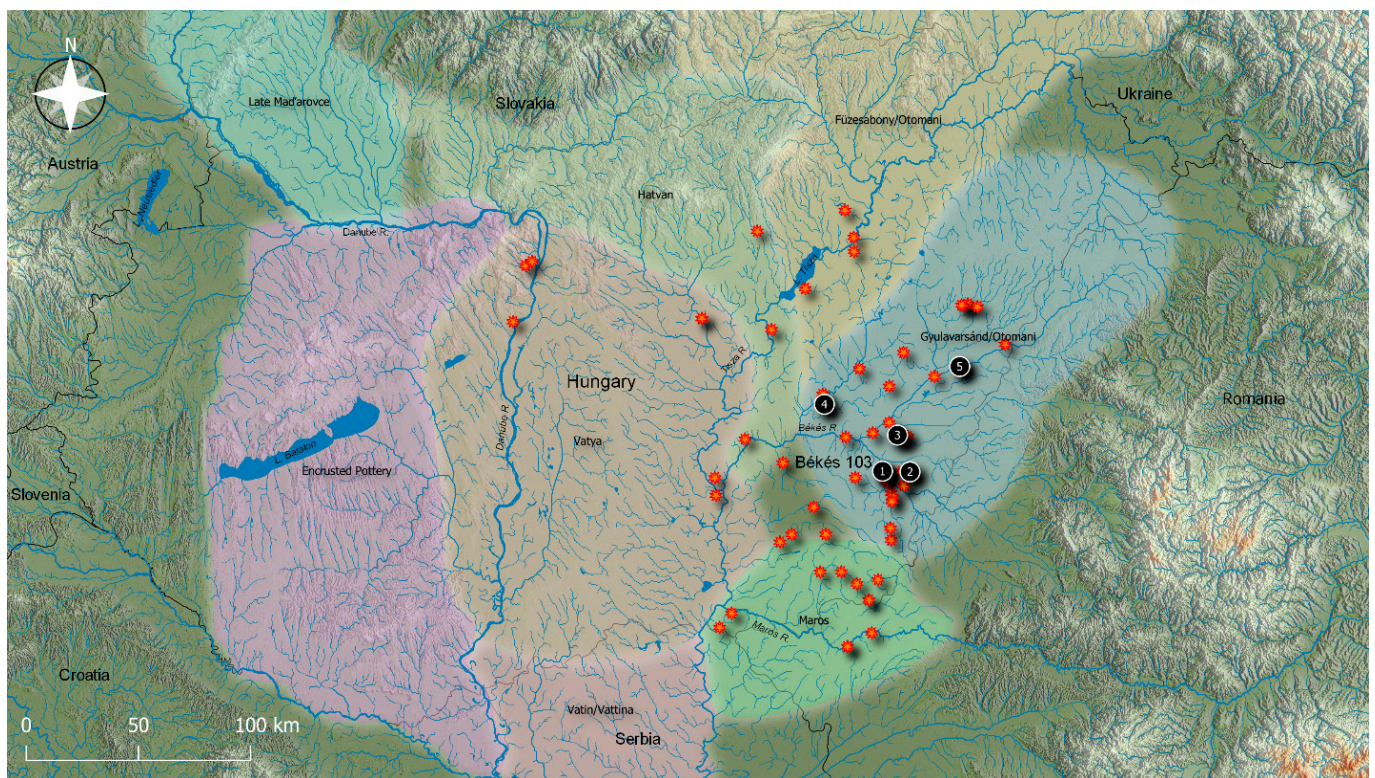


Figure 2. Map of the Carpathian Basin and surrounding regions showing major Middle Bronze Age stylistic/cultural units, and the location of sites from which ceramics were analyzed as part of the BAKOTA project. Sites: 1. Békés 103 (Jégvermi-kert) 2. Békés-Várdomb 3. Vésztő-Mágor 4. Túrkeve-Terehalom 5. Berettyóújfalu-Herpály. Clay sampling locations are indicated by red/orange stars. Culture/style areas redrawn after Fischl et al. [18].

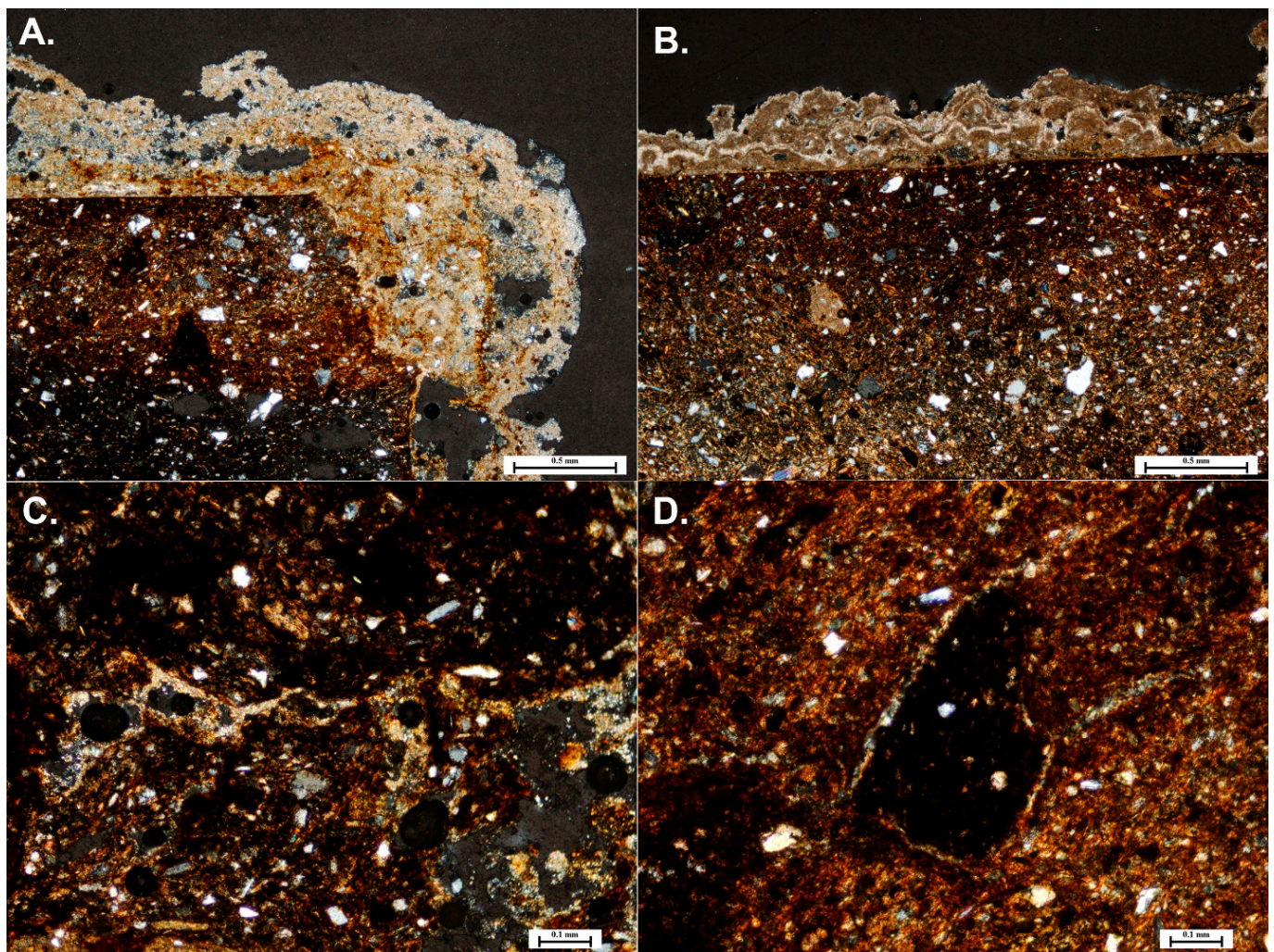


Figure 3. Thin-section micrographs (under crossed nichols) of selected sherds showing structure of surface encrustation and evidence for redeposited calcite along void and temper grain boundaries. (A) SS601; (B) SS592/593; (C) j24; (D) j29.

2. Materials and Methods

Our methodology was primarily devised to (1) determine the chemical and mineralogical composition of the surface encrustations on ceramics at Békés 103 and (2) determine whether potentially mobile elements may have been leached into or out of ceramics at the site. We also considered whether cremated remains and/or ash contained within burial urns may have contributed to the formation of surface encrustation and chemical alteration of paste composition. Data can be found in Tables S1–S3 (Supplementary Materials).

2.1. Sample

Our sample (Table 1) included 55 ceramic sherds selected either because they had particularly thick surface encrustations or because they had already been chemically measured by LA-ICP-MS. In the case of the latter ceramics, those analyzed prior to 2018 already had their surface encrustations removed prior to analysis and only retained small regions of remaining adhering crust. A set of surface collected sherds with particularly thick encrustations was initially selected (sample numbers starting with “ID” or “j”) for study, and were subsequently supplemented with sherds from burial vessels excavated and sampled during 2018, which were deliberately left uncleaned for this study. We also included 67 sediment samples from the site to examine the potential mobility of bone-derived elemental content into the surrounding burial soil. Ten of these samples were taken from beneath the plow zone (c. 1.5 m from surface) as far from any known burials as possible to assess baseline

soil chemistry at the site. The remaining 57 samples were collected from within burial pits in close association with vessel walls and associated cremated remains.

Table 1. Ceramic samples analyzed as part of this study, with applied methods indicated. Site phases are as follows—phase 1: c. 2460–2200 calBC; phase 3: c. 1880–1600 calBC; phase 4: c. 1600–1280 calBC; phase 5: c. 1280–1010 calBC [2]. (x) indicates that the referenced analysis method has been performed on the corresponding ceramic sample.

Sample	Context	Phase	Vessel Type	TS	PXRF	LA-ICP-MS	SEM-EDS	FT-IR
ID001	Cemetery				x			
ID002	Cemetery				x			
ID003	Cemetery				x			
ID004	Cemetery				x			
ID005	Cemetery				x			x
ID006	Cemetery				x			
ID007	Cemetery				x			
ID008	Cemetery				x			
ID009	Cemetery				x		x	x
ID010	Cemetery				x			
ID011	Settlement				x			
ID012	Cemetery				x		x	x
ID013	Settlement				x			
j29	Burial 6	4	jar/urn	x				
j37	Burial 2	4	jar/urn	x				
SS1071	Burial 70		jar/urn		x			
SS306	Burial 10	4	jar/urn		x			
SS325	Burial 20	4	jar/urn		x			
SS328	Burial 18	4	jar/urn		x			
SS407	Burial 24	4	pitcher/jug		x			
SS410	Burial 26	4	pitcher/jug		x			
SS416	Burial 34	4	cup/mug		x			
SS429	Burial 37	4	jar/urn		x			
SS435	Burial 23	4	jar/urn	x		x		
SS439	Burial 22	4	jar/urn	x	x	x	x	x
SS452	Burial 26	4	jar/urn		x			
SS471	Burial 34	4	jar/urn	x	x			
SS486	Burial 31		jar/urn		x			
SS511	Burial 28	4	jar/urn		x			
SS547	Burial 21	3	jar/urn		x			
SS555	Burial 31		pitcher/jug		x			
SS558	Burial 28	4	pitcher/jug		x			
SS572	Burial 13	4	jar/urn		x			
SS592/593	Burial 8	4	urn	x	x			
SS597	Burial 15	4	bowl		x			
SS601	Burial 8	4	bowl	x				
SS604	Burial 13	4	lid		x			
SS605	Burial 11	4	lid		x			
SS610	Burial 13	4	pitcher/jug		x			
SS614	Burial 14	3	bowl		x			
SS616	Burial 43	4	cup/mug		x			
SS618	Burial 28	4	bowl		x			
SS620	Burial 28	4	bowl		x			
SS692	Burial 52	3	cup/mug		x			
SS762	Burial 55	1	cup/mug		x			
SS782	Burial 57	5	cup/mug		x			
SS784	Burial 57	5	jar/urn		x			
SS815	Burial 59	5	pot/storage		x			
SS817	Burial 59	5	pot/storage		x			
SS818	Burial 59	5	cup/mug		x			
SS819	Burial 59	5	cup/mug		x			
SS919	Burial 33	4	bowl	x	x	x		
SS952	Burial 62	1	jar/urn		x			
SS955	Burial 66	4	jar/urn		x			

2.2. Methods

Thin-section petrography—As part of an earlier petrographic study of ceramics from the site, thin-sections were analyzed at the Hungarian National Museum using methods described by Kreiter [31]. The sample selected for that study only partially overlaps with subsequent chemical analyses. As part of this study, a number of vessel thin-sections were re-examined for the presence of residual surface encrustation and evidence of neo-formation or alteration of internal mineral content.

Fourier Transform Infrared Spectroscopy (FT-IR)—As a preliminary means of mineralogical characterization, surface encrustations from four sample vessels were analyzed by FT-IR [36] at the Field Museum of Natural History in Chicago. The Anthropological Conservation Laboratory there houses a Smiths IdentifyIR portable FT-IR instrument, a single bounce D-ATR FT-IR spectrometer with ZnSe beamsplitter, DTGS (deuterated-triglycine sulfate) detector, and sample press with LED display force indicator. Small amounts of surface encrustation were removed using a cleaned scalpel and pressed firmly against the instrument aperture for analysis. Resulting data were compared to relevant reference spectra obtained from the RRUFF (<https://rruff.info/>, accessed on 12 February 2021) database for peak identification.

X-ray Diffraction (XRD) and X-ray Photoelectron Spectroscopy (XPS)—Crust from a single sample (ID012) was analyzed by X-ray diffraction at the University of Notre Dame Materials Characterization Facility (Notre Dame, IN, USA) using a D8 Discover XRD spectrometer with Bruker Lynxeye detector. This sample was run without any preparation in standard Omega/2Theta geometry using the Cu K α line and was rotated to avoid the impact of any preferential crystal orientation. Peak identification was carried out by comparison to the International Centre for Diffraction Data database (<http://www.icdd.com/pdfsearch/>, accessed on 31 March 2021). As a compliment to XRD analysis, the same region of sample ID0012 was also characterized by XPS at the University of Notre Dame Materials Characterization Facility using a PHI VersaProbe II Ar ion gun.

Portable X-ray Fluorescence (PXRF)—All study samples were analyzed by PXRF at the University of Notre Dame Archaeological X-ray Laboratory (NDAXL, Notre Dame, IN, USA) using a Bruker Tracer 5i PXRF. Soil samples were finely powdered using an agate mortar, after which c. 5 g of material was placed into a plastic sample cup for analysis. Both surface and core paste measurements were taken on all ceramic samples. Samples were measured for 30 s apiece using the instrument's "Mudrock Dual" setting to quantify 21 major, minor, and trace elements. These values were then corrected against measurements of 13 NIST (679) and USGS (AGV-2, BCR-2, BHVO-2, BIR-1a, DNC-1a, DTS-2b, GSP-2, QLO-1a, RGM-2, SBC-1, SGR-1b, STM-2, W-2a) standards prepared either as loose powder (for soil samples) or pressed pellets (for ceramics). We measured New Ohio Red Clay (NORC) in both powdered and solid forms as a quality check standard. These values can be treated as quantitative for sediment samples, but given that the encrustation itself is of unknown composition, measurements on ceramic surfaces or directly on encrustation should be treated as semi-quantitative.

Scanning Electron Microscopy with Energy Dispersive Spectroscopy (SEM-EDS)—SEM-EDS imaging and analysis were performed at the University of Notre Dame Integrated Imaging Facility (Notre Dame, IN, USA) on a Magellan 400 XHR SEM with Bruker EDS array. After carbon sputter-coating, the paste-encrustation interface was imaged and analyzed on three different samples at 200 \times magnification using a 15 keV accelerating voltage to obtain data for elements between Mg and Ba.

Laser Ablation-Inductively Coupled Plasma-Mass Spectrometry (LA-ICP-MS)—Three ceramic sherds that had been previously analyzed—one with low Ba content (SS435), one with medium Ba content (SS439), and one with high Ba content (SS919)—were sectioned and analyzed by LA-ICP-MS at the Field Museum of Natural History Elemental Analysis Facility (EAF, Chicago, IL, USA). A raster of 100 μ m spots was ablated across each sherd using a NewWave UP213 laser ablation unit attached to a Thermo Quadrupole ICP-MS. Depending on sherd thickness, 50–160 individual spots were ablated to measure concen-

trations of 58 major, minor, and trace elements across each sample section (see [26] for a similar study). Data were calibrated using NIST610 and NIST679 standards with New Ohio Red Clay (NORC) run as a quality assurance check (see [37] for a detailed description of EAF instrumentation and methodology). Resulting data were input into ArcGIS10.5 and overlaid on sample images, after which interpolated concentration surfaces were generated for potentially mobile elements (P, Ca, Sr, Ba) using an inverse distance weighting (IDW) algorithm.

3. Results

3.1. Crust Composition

In thin-section, the complex and layered structure of the surface encrustation is clearly visible (Figure 3). On sample SS601 (part of a shallow bowl from an MBA burial), the encrustation clearly covers both the original surface of the vessel as well as an old break (to the right of the figure). The encrustation contains numerous semiangular quartz grains as well as dark opaque minerals (likely hematite). These mineral grains appear more abundant in the inner layer of the crust in this particular case, while the outer regions of the crust are more texturally homogenous. In both this image and on sample SS592/593 (part of a large MBA burial urn), voids lined with fine calcite crystals appear throughout the encrustation. The crust on SS592/593 is quite visually different from that on SS601, however, as it clearly contains a higher density of yellow-brownish material possibly composed of phosphates and/or soil clay minerals containing distinct wavy bands of calcite crystals. There is also a small fragment of pottery embedded within the crust, likely a piece of the vessel itself that has broken free and has been surrounded by the encrustation.

The elemental content of the surface encrustations was estimated using a combination of XRF, SEM-EDS, and LA-ICP-MS measurements. In the case of XRF analysis, it was not possible to fully control for the contribution of underlying paste composition as the penetration depth of incident X-rays cannot be altered or controlled. SEM-EDS was performed on cut sherd cross-sections for three samples (ID005, ID012, and SS439) chosen because they had particularly thick surface encrustations. LA-ICP-MS measurements were obtained on a small region of encrustation on sample SS435 during raster mapping. SEM-EDS measurements (Figure 4) clearly demonstrate that the crust is highly enriched in calcium and carbon relative to underlying paste, further indicating that calcite is the primary constituent. Elevated phosphorus concentrations (not shown) were also observed in two of the three samples (ID012 and SS439), but are not evident in ID005. PXRF (Figure 5) analysis (sampling a far larger region of crust) likewise indicates moderate elevation of P concentrations on most vessel surfaces, indicating that phosphates such as apatite could form part of the encrustation. Mn and Fe are moderately enriched in surface compared to paste measurements, consistent with macro- and microscopic identification of hematite and other opaque mineral phases. Their presence is not surprising as both elements are mobile in groundwater and particularly prone to buildup under reducing soil conditions, for instance during periods of high soil moisture [35], but could also be present in the form of iron phosphates such as vivianite or anapaite [38]. LA-ICP-MS measurements on sample SS435 indicate that the encrustation is additionally substantially enriched in Mg, Cl, and As, and slightly enriched in Ba and Pb when compared to measurements on nearby regions of paste.

FT-IR results (Figure 6) confirm the presence of calcite (wavenumbers 1424, 876, 712) [39–41] and indicate the presence of phosphates (wavenumber 1020) in all four analyzed samples. There is a weak nitrate peak (possibly cyanamide) in some of the samples as well (an element not measured by XRF or LA-ICP-MS), but this is clearly a very minor constituent. The absorbance spectra for samples ID005 and ID009 are nearly identical, with tall calcite peaks and relatively lower phosphate peaks, while samples ID012 and SS439 exhibit relatively larger phosphate peaks. These differences likely relate to areal variance in crust composition rather than indicating any systematic difference in crust composition

between these samples, which are otherwise relatively similar in appearance and bulk chemical composition.

XRD analysis (Figure 7) of the surface of sample ID012 likewise shows that calcite comprises the primary component of the surface encrustation on this vessel. The XRD spectra also show the presence of quartz, as identified in thin-section micrographs. Apatite peaks are evident but are relatively weak, further indicating that phosphates form a relatively minor component of the surface encrustation. That said, the observed heterogeneity of the surface encrustation as evident in thin-section also suggests that individual surface XRD measurements may miss some components of the encrustation while identifying others, or that the relative contributions of different phases are likely highly variable spatially in the encrustation.

XPS analysis of sample ID012 (Figure 8) likewise indicates the presence of calcite (347.0 eV), but also calcium nitrate (350.5 eV), silicates (102.3 eV), aluminum oxides (531.3 eV), iron oxides and possibly phosphates, including possible metaphosphate (phosphate-oxide, 134.9 eV), hydroxyfluoroapatite (684.5 eV), and possibly magnesium fluoride (686.1 eV). Also present are a variety of organic compounds including aromatics (peak at 283.7 eV), carboxyls (285 eV), carbonates (289.6 and 292.8 eV), and phenyl ether (294.4 eV).

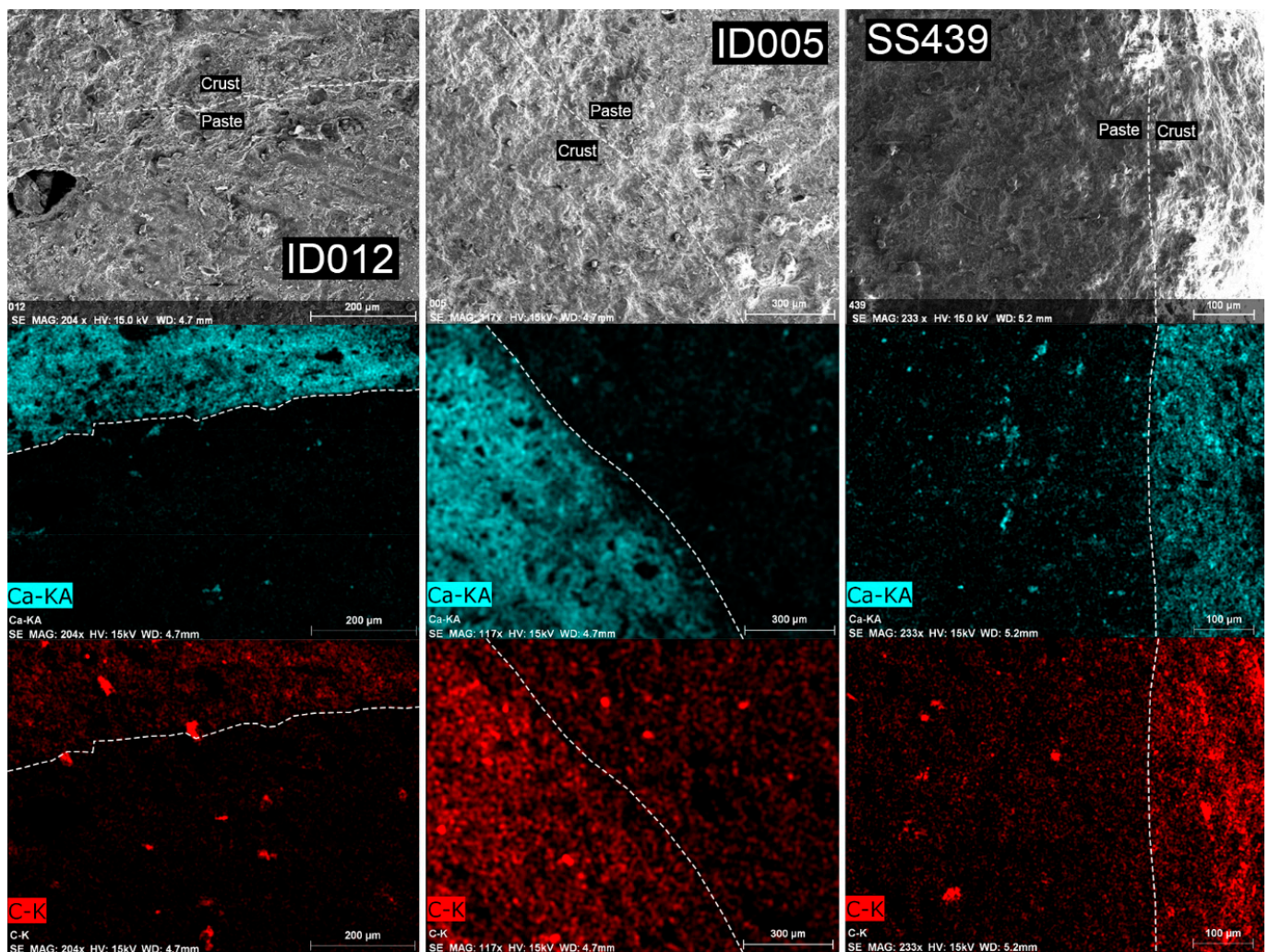


Figure 4. SEM images of the paste/crust boundary in three samples (ID012, ID005, and SS439), with SEM-EDS false color images of Ca and C concentrations. Lighter colors indicate higher peak intensity.

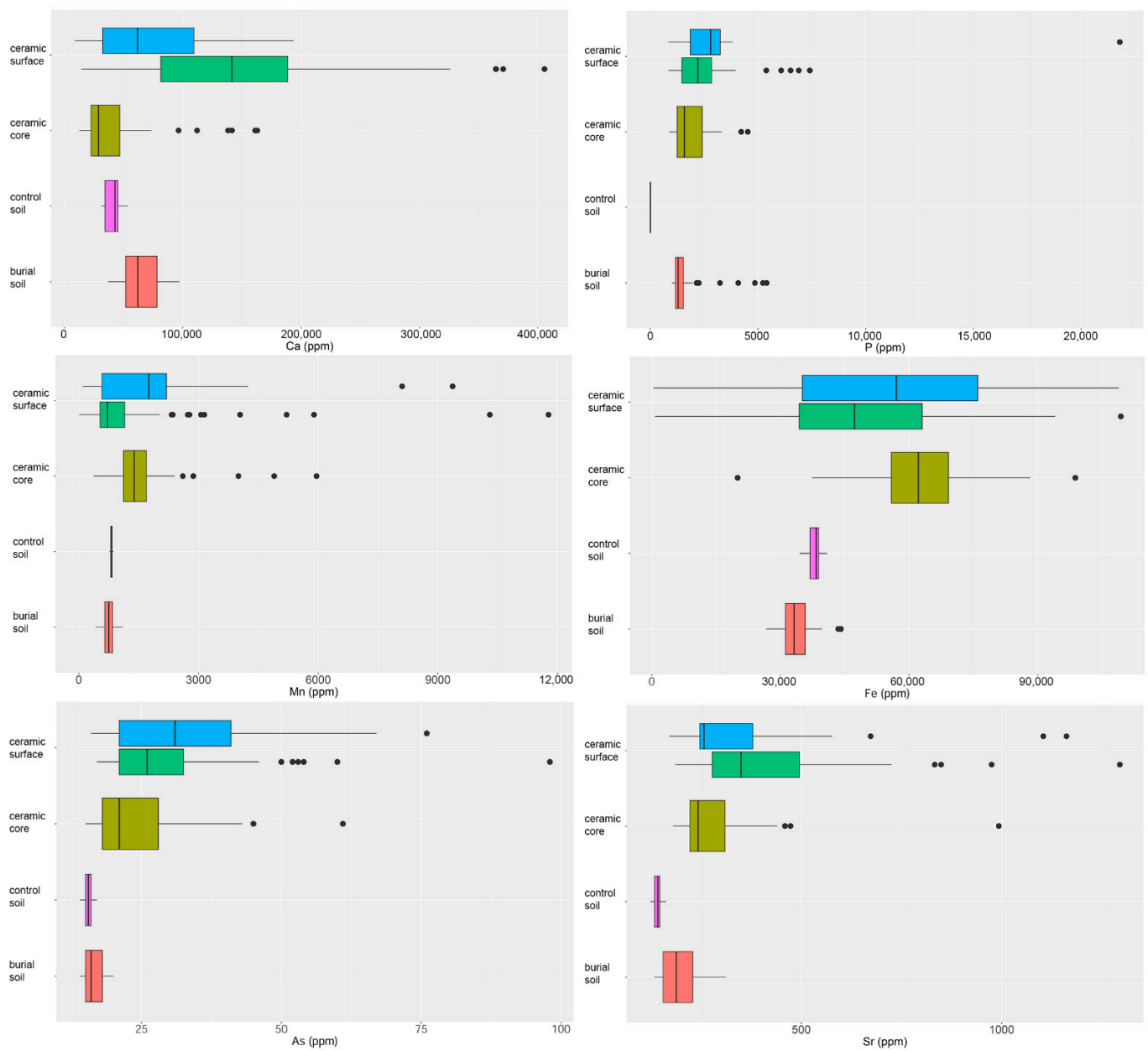


Figure 5. Box-and-whisker plots of selected elemental concentrations measured by PXRF on vessel surfaces (blue, without visible crust; green, with visible crust), vessel cores/cross-sections, control soil samples, and burial soil samples.

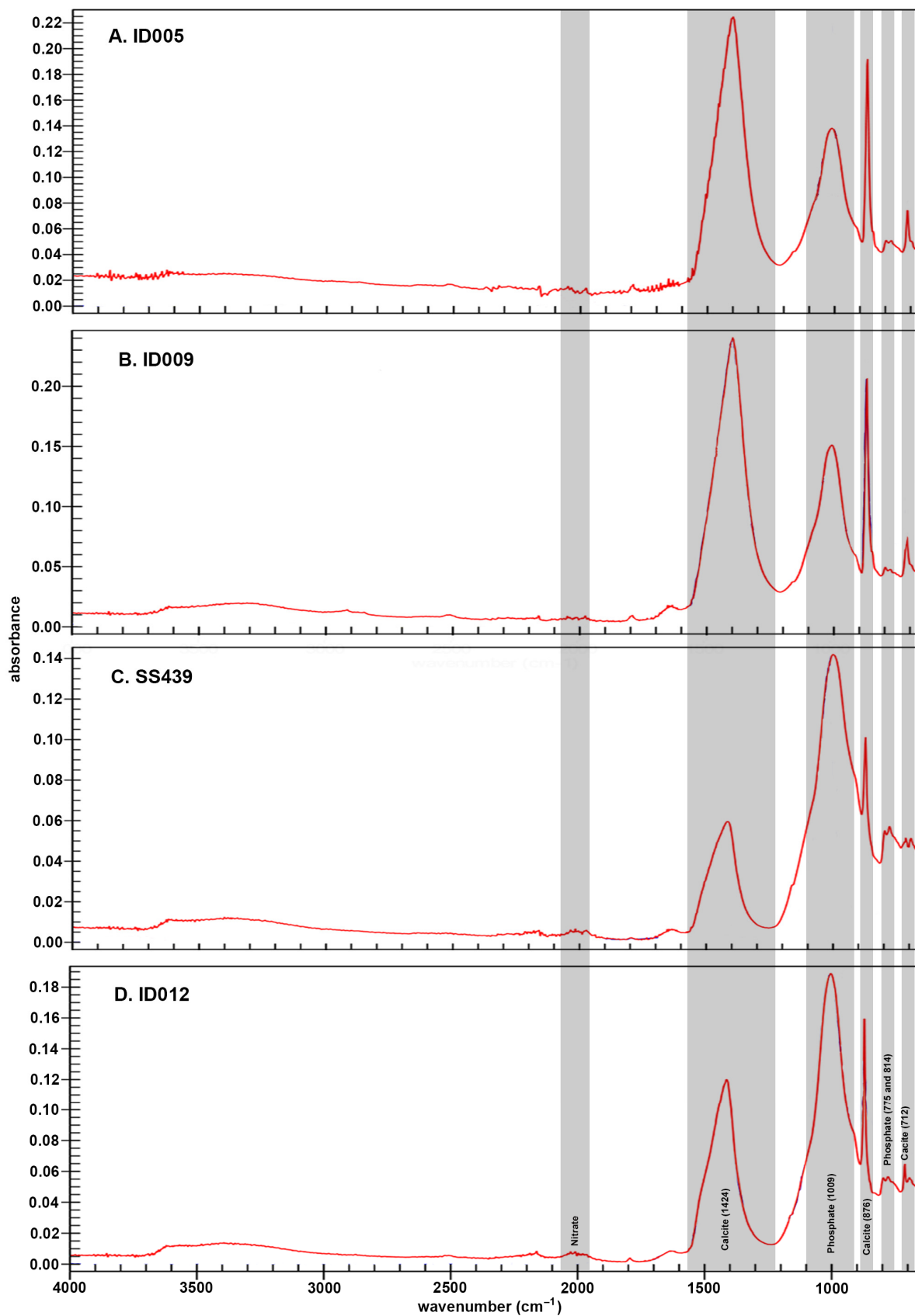


Figure 6. FT-IR absorbance spectra for crust samples with relevant peak areas indicated.

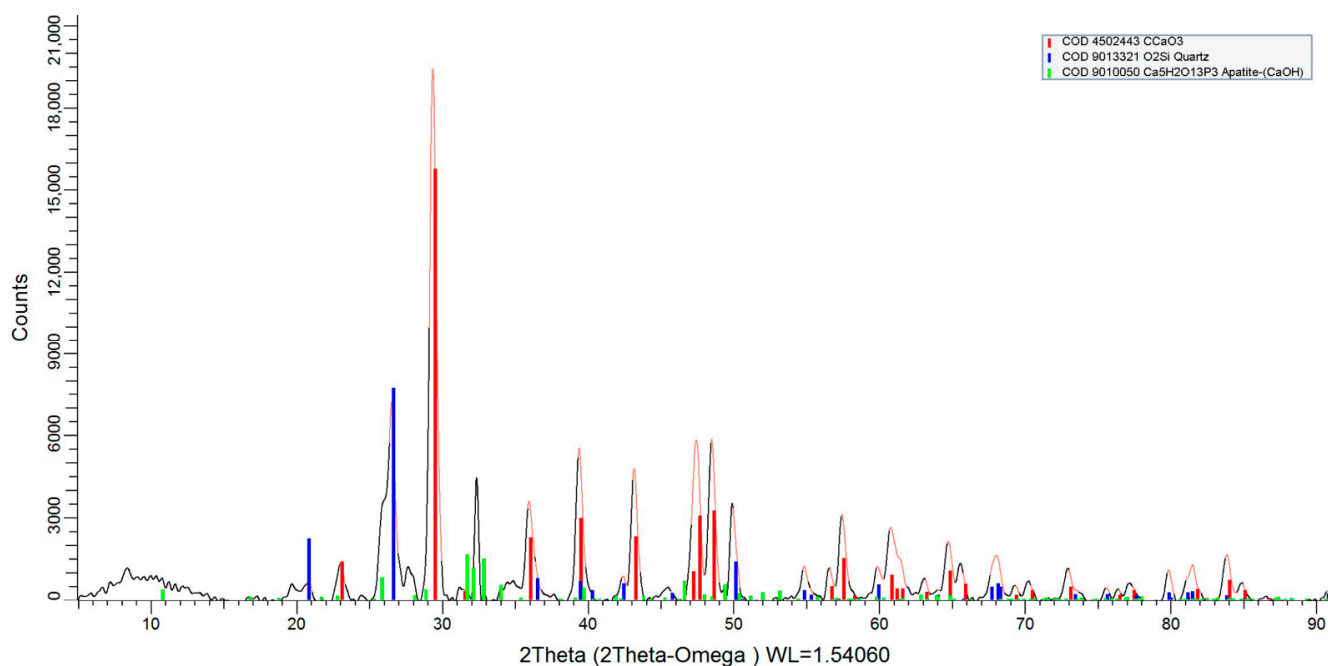


Figure 7. XRD spectrum for encrustation on the external surface of sample ID012 with reference peaks for calcite (red), quartz (blue), and apatite (green) indicated.

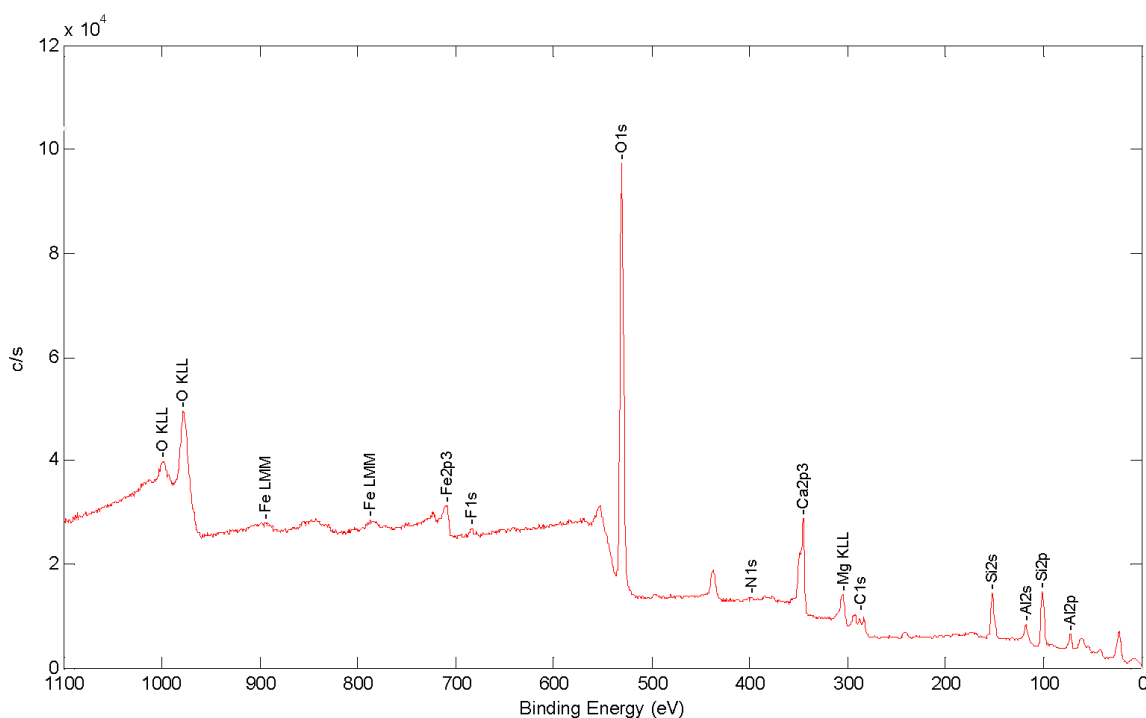


Figure 8. XPS spectrum for encrustation on the external surface of sample ID012 with peaks identified.

3.2. Identification of Elemental Leaching

Redeposited calcite is abundantly evident in thin-section micrographs (Figure 3C,D), lining the edges of pores and voids as well as gaps around larger inclusions. As calcite is soft and often destroyed during production of thin-sections, it is likely that the images presented here underestimate the degree to which redeposited calcite is present in sherds from Békés 103. Calcite may of course derive from calcium and carbon-rich phases initially present in the ceramic such as bone or shell [38], but there is little evidence that deliberate

addition of such temper was practiced in the Otomani–Gyulavarsánd ceramic tradition. Micritic carbonate is naturally present in some local sediments and clays, and is sometimes present as visible distinct inclusions within ceramic pastes [31]. It is possible that some calcite derives from dissolved and redeposited micritic carbonate, but this is unlikely to account for the volume of material deposited on sherd surfaces. It seems more likely that the majority of neo-formed calcite derives from the burial environment.

Interpolated elemental maps produced by LA-ICP-MS rastering support this interpretation—Ca concentrations tend to be higher near vessel walls and around major pores, voids, and larger temper grains. Rastering also indicates that numerous other mobile elements have been variably enriched (Figure 9). Sample SS435 (originally measured at an average Ba content of 552 ppm) shows relatively little evidence for leaching of elemental content into the paste, with relatively low and uniform Ca, P, Sr, and Ba concentrations away from the vessel surface, where the laser ablated small areas of remaining encrustation. There are, however, localized “hotspots” near the center of the sherd associated with a large void that runs diagonally across the sherd cross-section. SS439 (measured average Ba content 644 ppm) likewise has localized areas of elevated concentrations for all three elements near the vessel walls but also shows substantially elevated concentrations of mobile elements around a clay pellet surrounded by a large void. Enrichment is most evident for P, but all four elements displayed here show some degree of enrichment in this area of the sherd cross-section. Sample SS919, which had the highest measured Ba content (1014 ppm) of any vessel included in the original LA-ICP-MS analysis, shows a clear enrichment of mobile elements toward the outer vessel wall and extending nearly to the center of the sherd. Even away from this localized enrichment, baseline values of these elements are higher than in SS435 or SS439. Whether this indicates a general enrichment of values across the entirety of the profile in SS919 or higher initial concentrations of these elements is unclear.

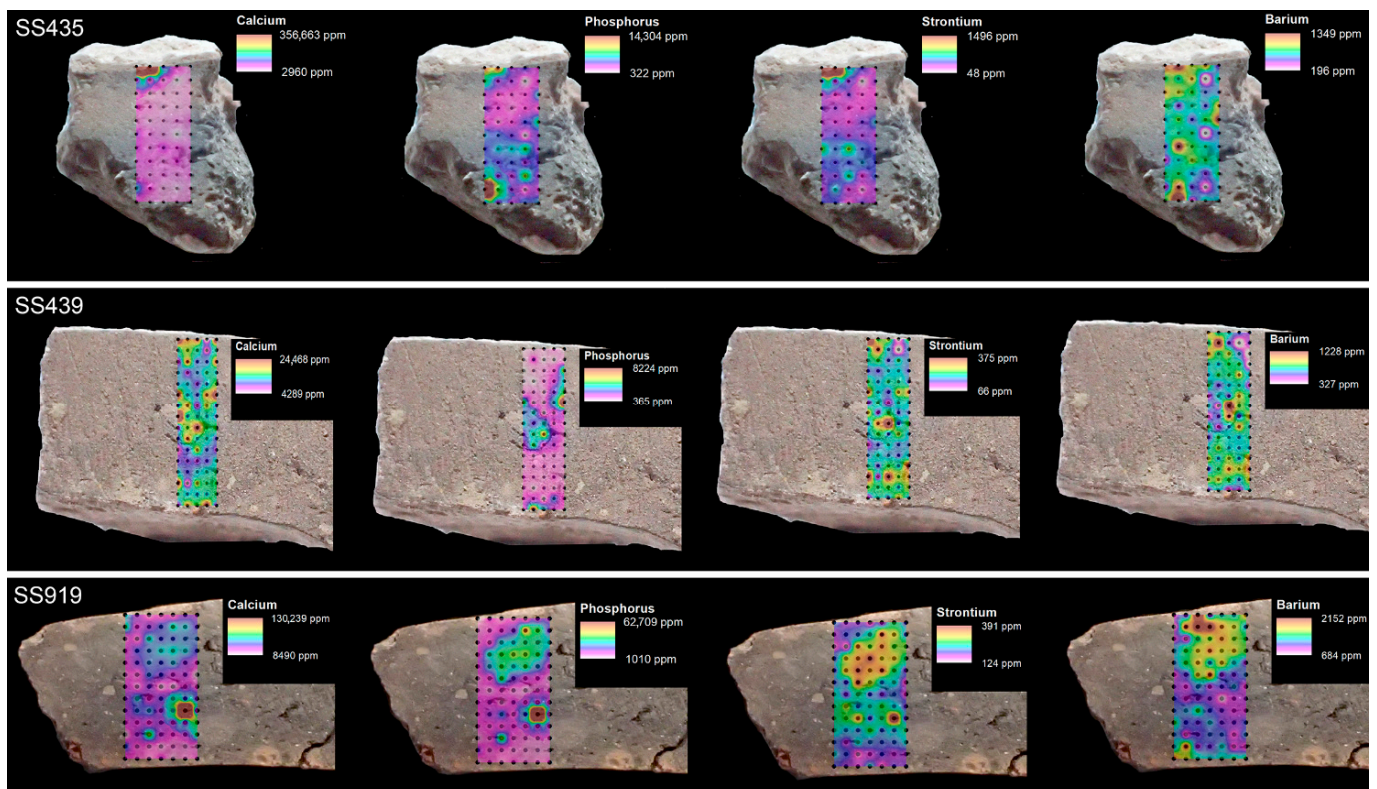


Figure 9. Contour plots of elemental (Ca, P, Sr, Ba) content in sherd cross-sections for samples SS435, SS439, and SS919. Contours generated by the Inverse Distance Weighting algorithm in ArcGIS10.5.1. Ablation spots are indicated with black dots; all values are expressed in parts per million.

These values can be compared to those measured in clays sampled from across the GHP. While certain calcareous/marly clays have measured Ca and Sr concentrations comparable to those present in sherd cross-sections, these clays proved largely unsuitable for ceramic production. The Ba values measured in sherds SS439 and SS919 in particular are well beyond the values obtained in any sampled clays, for which the maximum measured concentration was 687 ppm (average c. 450 ppm). Note that other elements identified as potentially mobile and elevated in the surface encrustation (Mg, Pb) also mimic patterns of the four elements shown here, suggesting that the principal constituents of the surface encrustation have all impacted internal paste composition to a greater or lesser degree. It is not certain why some sherds were more impacted than others, but in addition to differences in the localized burial environment (e.g., soil moisture, local variance in pH and redox conditions, depth, and so forth), differences in the degree of surface burnishing and paste composition (fewer or more voids or inclusions) may play a role in making some vessels more susceptible to leaching than others [26,42–46]. Even so, it seems probable that most of the sherds recovered from the site have been impacted to one degree or another by post-burial leaching of mobile elements.

4. Discussion

In summary, the encrustations on vessels from Békés 103 are primarily composed of neo-formed calcite with a minor presence of phosphates (including apatite), nitrates, and a variety of other mineral types including quartz, mica and hematite, and organic compounds. This composition points to uptake and deposition of dissolved carbonates and phosphates from the surrounding burial environment as well as other organic and inorganic soil components that have been cemented to the vessel surface as part of the surface encrustation. Given the seasonal soaking and drying that occurs in regional sediments, particularly prior to the canalization of rivers and draining of local swamps, it is perhaps not surprising that ceramics at the site have been heavily impacted by elemental mobility and deposition of soil-derived minerals. The structured and partially layered appearance of the crust suggests a progressive buildup during periods of peak soil moisture, but this likely was also complex and involved frequent recrystallization of carbonates and phosphates on the surface that have resulted in a complexly layered and spatially heterogeneous structure. Groundwater also carried a suite of mobile elements into the ceramic paste, where Ca at least recrystallized around pore boundaries and in voids as substantial deposits of calcite. SEM-EDS imaging of pore boundaries and near vessel surfaces failed to detect discrete phases containing other mobile elements (Ba, Sr), suggesting that these elements are more likely to have bonded with clay minerals within the paste rather than forming discrete mineral phases such as barite or strontianite.

While carbonates and phosphates originally derived from the surrounding soil matrix are likely to represent the principal source of elemental uptake and deposition [38], the presence of large amounts of human bone in proximity to most of the ceramics at Békés 103 allows for the possibility that bone and/or bone ash might also have contributed. In a recent study of Shimotabaru ceramics from the Ryukyu Islands (Japan), Aoyama et al. [47] demonstrate leaching of elemental content from faunal remains at the site and deposition onto vessel surfaces as a whitish-grey surface encrustation that is visually similar to that found on ceramics at Békés 103. The total absence of bone ash in burial urns at the site remains a mystery, as even very delicate bone fragments (orbital bones from child burials, for instance) are present. Typically, removal of bones from cremation pyres results either in retention of only larger and more robust bone fragments, or inclusion of large amounts of bone ash and wood ash and charcoal in the burial urn. As such, it is possible that bone ash and/or dissolved bone might have contributed to the ceramic surface encrustations, particularly as bone is principally composed of or may contain exactly the elements that are enriched in the surface encrustations and paste—C, Mg, P, Ca, As, Sr, Ba, and Pb.

Recent experimental studies suggest that fully calcined cremated bone may be more resistant to diagenesis than unburnt or charred bone due to recrystallization of bioapatite into less reactive hydroxyapatite [48–50]. FT-IR analysis of cremated samples from Békés 103 burials suggests a significant degree of calcination, indicating likely firing temperatures of 600 to 800 °C, but with only minimal change in crystallinity index between non-calcined and heavily calcined samples [51]. Studies of bone diagenesis further suggest that alteration is highly dependent on soil pH, redox conditions, and moisture exposure and variability [26,42–46]. Prior experimental studies suggest that bone is most susceptible to breakdown at pH values below six or above nine [43,44]. Published geochemical measurements (FOREGS database) indicate that subsoil values in the Békés area are neutral to moderately acidic (5.0–6.0) [52]. Direct measurement of pH in control and burial samples (using litmus paper test strips) indicate more basic values of 7.5–8.5, similar to values measured from settlement contexts at nearby non-tell sites from the Neolithic, Copper, and Bronze ages (6.0–8.2) [53]. Nonetheless, the skeletal material at Békés 103 is only partially calcined and has clearly been subjected to an aggressive burial environment for millennia, suggesting that bone diagenesis is highly likely. XRF analyses of sediment samples indicate elevated concentrations of mobile elements, including Ca and P in burial sediments, when compared to control samples (Figure 5), suggesting that at least some material from cremated remains has been mobilized in the soil. Burial soils were moderately more basic than control samples as well, possibly as a result of introduction of dissolved alkaline elements into the surrounding sediment. Further mineralogical and chemical examination of cremated remains from the site will be needed to shed further light on this issue.

5. Conclusions

This study documents the deposition of neo-formed calcite on ceramics from the Bronze Age site of Békés 103. The material is, however, highly heterogeneous and also contains quartz and other mineral grains derived from surrounding sediment as well as other calcium-rich phosphate phases that are variously distributed. This crust is almost certainly a result of millennia of burial in an environment characterized by high but seasonally variable soil moisture, which has mobilized a number of alkaline-earth elements as well as P, As, and Pb. Groundwater has also clearly permeated vessel walls, and both formed visible secondary calcite along pores, voids, and temper grain edges, as well as leaching other mobile elements into the vessel paste.

While it is possible to mechanically remove the surface crust, reconstructing the original pre-burial chemical composition of these sherds is far more challenging. Minimally, mobile elements identified in this study will need to be removed from consideration during further compositional analysis of ceramics from the site. Given similar conditions in many parts of the GHP/Pannonian Basin, it is likely that ceramics from other sites are similarly impacted, and any future compositional analyses in the region will need to take into account the impacts of post-burial alteration. Furthermore, it is likely that elemental mobility has not just impacted ceramics. Similar detailed diagenetic examination of human remains from flat sites on the Great Hungarian Plain should be carried out prior to conducting isotopic studies (e.g., [54]) using mobile elements (C, N, P, and Sr). Archaeologists investigating materials from low-lying, seasonally inundated contexts outside the study region likely also must contend with potential alterations of the kind reported here.

Supplementary Materials: The following are available online at <https://www.mdpi.com/article/10.3390/min11040436/s1>. Table S1: XRF measurements for all ceramic and soil samples included in the study. Values are reported in parts per million, Table S2: XRD peak intensities, in counts per second, Table S3: LA-ICP-MS raster measurements, values expressed in parts per million.

Author Contributions: Conceptualization, M.G., A.M., P.R.D., G.M.P. and J.I.G.; methodology, M.G., A.M., I.V.L., P.R.D., G.M.P., A.K. and J.I.G.; software, M.G.; validation, M.G., A.K. and I.V.L.; formal analysis, M.G. and A.K.; investigation; M.G., A.M., A.K. and I.V.L.; resources, M.G., A.K. and I.V.L.; data curation, M.G., J.I.G., P.R.D. and G.M.P.; writing—original draft preparation, M.G. and A.M.; writing—review and editing, P.R.D., G.M.P., A.K., I.V.L. and J.I.G.; visualization, M.G., A.K. and I.V.L.; supervision, M.G., P.R.D., G.M.P. and J.I.G.; project administration, M.G., P.R.D., G.M.P. and J.I.G.; funding acquisition, J.I.G., P.R.D., G.M.P., I.V.L. and M.G. All authors have read and agreed to the published version of the manuscript.

Funding: The United States National Science Foundation (grants BCS1460820 and BCS1628026) and the University of Notre Dame funded this research.

Data Availability Statement: XRF, XRD, and LA-ICP-MS measurements are available in supplemental Tables S1–S3.

Acknowledgments: We would like to thank Tatyana Orlova, Alexander Mukasyan, Laure Dussubieux, Beth Grávalos, Craig Jenson, and J.P. Brown for their assistance with various analyses reported here. Several anonymous reviewers provided helpful comments that contributed greatly to improving earlier versions of this paper.

Conflicts of Interest: The authors declare no conflict of interest.

References

- Neff, H.; Cogswell, J.W.; Ross, L.M.J. Supplementing bulk chemistry in archaeological provenience investigations. In *Patterns and Process: A Festschrift in Honor of Dr. Edward V. Sayre*; van Zelst, L., Ed.; Smithsonian Center for Materials Research and Education: Suitland, MD, USA, 2003; pp. 200–224.
- Duffy, P.R.; Parditka, G.M.; Giblin, J.I.; Paja, L. The problem with tells: Lessons learned from absolute dating of Bronze Age mortuary ceramics in Hungary. *Antiquity* **2019**, *93*, 63–79. [[CrossRef](#)]
- Duffy, P.R. River networks and funerary metal in the Bronze Age of the Carpathian Basin. *PLoS ONE* **2020**, *15*, e0238526. [[CrossRef](#)] [[PubMed](#)]
- Duffy, P.R.; Paja, L.; Parditka, G.M.; Giblin, J.I. Modelling mortuary populations at local and regional levels. *J. Anthr. Archaeol.* **2019**, *53*, 240–261. [[CrossRef](#)]
- Duffy, P.R.; Parditka, G.M.; Giblin, J.I.; Paja, L.; Salisbury, R.B. Discovering Mortuary Practices in the Körös River Basin, Hungary. *Hung. Archaeol. E-J. Magy. Régészet Online Mag.* **2014**, *Autumn*, 1–5.
- Paja, L.; Duffy, P.R.; Parditka, G.M.; Giblin, J.I. Bioanthropological analysis of Békés 103 (Jégvermi-kert, Lipscei-tanya), a Bronze Age cemetery from southeastern Hungary. *Acta Biol. Szeged.* **2016**, *60*, 183–192.
- O’Shea, J.M. *Villagers of the Maros: A Portrait of an Early Bronze Age Society*; Plenum Press: New York, NY, USA, 1996.
- Riebe, D.J.; Duffy, P.R. Baroque by whose hand? Detailing the regional production of finewares in Middle Bronze Age Hungary. Paper Presented at the 79th Annual Meeting of the Society for American Archaeology, Austin, TX, USA, 23–27 April 2014.
- Parkinson, W.A.; Palmer, R.A.; Xia, Y.; Carlock, B.; Gyucha, A.; Yerkes, R.W.; Galaty, M.L. Elemental analysis of ceramic incrustation indicates long-term cultural continuity in the prehistoric Carpathian Basin. *Archaeol. Ethnol. Anthropol. Eurasia* **2010**, *201038*, 64–70. [[CrossRef](#)]
- Odrizola, C.P.; Hurtado Pérez, V.M. The manufacturing process of 3rd millennium BC bone based incusted pottery decoration from the Middle Guadiana river basin (Badajoz, Spain). *J. Archaeol. Sci.* **2007**, *34*, 1794–1803. [[CrossRef](#)]
- Všianský, D.; Kolář, J.; Petřík, J. Continuity and changes of manufacturing traditions of Bell Beaker and Bronze Age encrusted pottery in the Morava river catchment (Czech Republic). *J. Archaeol. Sci.* **2014**, *49*, 414–422. [[CrossRef](#)]
- Hajdu, T.; György-Toronyi, A.; Pap, I.; Rosendahl, W.; Szabó, G. The chronology and meaning of the Transdanubian encrusted pottery decoration. *Praehist. Z.* **2016**, *91*, 353–368. [[CrossRef](#)]
- Kiss, V. *Middle Bronze Age Encrusted Pottery in Western Hungary*; Archaeolingua: Budapest, Hungary, 2012.
- Roberts, S.; Sofaer, J.; Kiss, V. Characterization and textural analysis of Middle Bronze Age Transdanubian inlaid wares of the Encrusted Pottery Culture, Hungary: A preliminary study. *J. Archaeol. Sci.* **2008**, *35*, 322–330. [[CrossRef](#)]
- Sofaer, J.; Mihelić, S. Pattern, colour, and texture in encrusted ceramics in the Carpathian Basin. In *Creativity in the Bronze Age: Understanding Innovation in Pottery, Textile, and Metalwork Production*; Jørgensen, L.B., Sofaer, J., Stig Sørensen, M.L., Eds.; Cambridge University Press: Cambridge, UK, 2018; pp. 263–274.
- Sziki, G.A.; Biró, K.T.; Uzonyi, I.; Dobos, E.; Kiss, A.Z. Investigation of incusted pottery found in the territory of Hungary by micro-PIXE method. *Nucl. Instrum. Methods Phys. Res. Sect. B Beam Interact. Mater. At.* **2004**, *210*, 478–482. [[CrossRef](#)]
- Stig Sørensen, M.L.; Rebay-Salisbury, K. Landscapes of the Body: Burials of the Middle Bronze Age in Hungary. *Eur. J. Archaeol.* **2009**, *11*, 49–74. [[CrossRef](#)]

18. Fischl, K.P.; Kiss, V.; Kulcsár, G.; Szeverényi, V. Transformations in the Carpathian Basin around 1600 B.C. In *1600—Cultural Change in the Shadow of the Thera-Eruption? Tagungen des Landesmuseums für Vorgeschichte Halle (9)*; Meller, H., Bertemes, F., Bork, H.-R., Risch, R., Eds.; Landesamt für Denkmalpflege und Archäologie Sachsen-Anhalt - Landesmuseum für Vorgeschichte, Halle: Halle (Saale), Germany, 2013; Volume 9, pp. 355–370.
19. Sofaer, J. Cosmologies in clay: Swedish Helmet Bowls in the Middle Bronze Age of the Carpathian Basin. In *Counterpoint: Essays in archaeology and heritage studies in honour of Professor Kristian Kristiansen*; Bergerbrant, S., Sabatini, S., Eds.; BAR International Series 2508; Archaeopress: Oxford, UK, 2013; pp. 361–365.
20. Casaletto, M.P.; Ingo, G.M.; Riccucci, C.; De Caro, T.; Bultrini, G.; Fragalà, I.; Leoni, M. Chemical cleaning of encrustations on archaeological ceramic artefacts found in different Italian sites. *Appl. Phys. A* **2008**, *92*, 35–42. [[CrossRef](#)]
21. Gyucha, A.; Duffy, P.R.; Frolking, T.A. The Körös Basin from the Neolithic to the Hapsburgs: Linking Settlement Distributions with Pre-Regulation Hydrology through Multiple Data Set Overlay. *Geoarchaeology* **2011**, *26*, 392–419. [[CrossRef](#)]
22. Duffy, P.R. *Complexity and Autonomy in Bronze Age Europe: Assessing Cultural Developments in Eastern Hungary. Prehistoric Research in the Körös Region*; Archaeolingua: Budapest, Hungary, 2014.
23. Dunnell, R.C.; Hunt, T.L. Elemental composition and inference of ceramic vessel function. *Curr. Anthropol.* **1990**, *31*, 330–336. [[CrossRef](#)]
24. Franklin, U.M.; Vitali, V. The environmental stability of ancient ceramics. *Archaeometry* **1985**, *27*, 3–15. [[CrossRef](#)]
25. Freestone, I.C.; Meeks, N.D.; Middleton, A.P. Retention of phosphate in buried ceramics: An electron microbeam approach. *Archaeometry* **1985**, *27*, 161–177. [[CrossRef](#)]
26. Golitko, M.; Dudgeon, J.V.; Neff, H.; Terrell, J.E. Identification of post-depositional chemical alteration of ceramics from the north coast of Papua New Guinea (Sanduan Province) by time-of-flight-laser ablation-inductively coupled plasma-mass spectrometry (TOF-LA-ICP-MS). *Archaeometry* **2012**, *54*, 80–100. [[CrossRef](#)]
27. Heinmann, R.B. Firing technologies and their possible assessment by modern analytical methods. In *Archaeological Ceramics*; Olin, J.S., Franklin, J.D., Eds.; Smithsonian Institution: Washington, DC, USA, 1982; pp. 86–96.
28. Maggetti, M. Phase analysis and its significance for technology and origin. In *Archaeological Ceramics*; Olin, J.S., Franklin, J.D., Eds.; Smithsonian Institution: Washington, DC, USA, 1982; pp. 121–134.
29. Picon, M. Quelques observations complémentaires sur les alterations de composition des céramiques au cours du temps: Cas de quelques alcalins et alcalino-terreux. *ArchéoSciences revue d'Archéométrie* **1991**, *11*, 41–47. [[CrossRef](#)]
30. Hedges, R.E.M.; McLellan, M. On the cation exchange capacity of fired clays and its effects on the chemical and radiometric analysis of pottery. *Archaeometry* **1976**, *18*, 203–207. [[CrossRef](#)]
31. Kreiter, A. *Technological choices and material meanings: Analyses of Early and Middle Bronze Age ceramics from Hungary*; BAR International Series 1604; Archaeopress: Oxford, UK, 2007.
32. Kreiter, A.; Bajnóczy, B.; Sipos, P.; Szakmány, G.Y.; Tóth, M. Archaeometric examination of Early and Middle Bronze Age ceramics from Százhalombatta-Földvár, Hungary. *Archeometriai Műhely* **2007**, *2007*, 33–47.
33. Maniatis, Y.; Tite, M.S. Technological examination of Neolithic-Bronze Age pottery from Central and Southeastern Europe and from the Near East. *J. Archaeol. Sci.* **1981**, *8*, 59–76. [[CrossRef](#)]
34. Michelaki, K. Making Pots and Potters in the Bronze Age Maros Villages of Kiszombor-Új-Élet and Klárafalva-Hajdova. *Camb. Archaeol. J.* **2008**, *18*, 355–380. [[CrossRef](#)]
35. Maritan, L. Ceramic abandonment. How to recognise post-depositional transformations. *Archaeol. Anthropol. Sci.* **2020**, *12*, 199. [[CrossRef](#)]
36. Shoval, S. Fourier Transform Infrared Spectroscopy (FT-IR) in Archaeological Ceramic Analysis. In *The Oxford Handbook of Archaeological Ceramic Analysis*; Hunt, A.M.W., Ed.; Oxford University Press: Oxford, UK, 2017; pp. 509–530.
37. Golitko, M. *LBK Realpolitik: An Archaeometric Study of Conflict and Social Structure in the Belgian Early Neolithic*; Archaeopress: Oxford, UK, 2015.
38. Maritan, L.; Mazzoli, C. Phosphates in archaeological finds: Implications for environmental conditions of burial. *Archaeometry* **2004**, *46*, 673–683. [[CrossRef](#)]
39. Bosch Reig, F.; Gimeno Adelantado, J.V.; Moya Moreno, M.C.M. FTIR quantitative analysis of calcium carbonate (calcite) and silica (quartz) mixtures using the constant ratio method. Applications to geological samples. *Talanta* **2002**, *58*, 811–821.
40. Neff, H.; Bigney, S.J.; Sakai, S.; Burger, P.R.; Garfin, T.; George, R.G.; Cullteon, B.J.; Kennett, D.J. Characterization of Archaeological Sediments Using Fourier Transform Infrared (FT-IR) and Portable X-ray Fluorescence (pXRF): An Application to Formative Period Pyro-Industrial Sites in Pacific Coastal Southern Chiapas, Mexico. *Appl. Spectrosc.* **2016**, *70*, 110–127. [[CrossRef](#)]
41. Regev, L.; Poduska, K.M.; Addadi, L.; Weiner, S.; Boaretto, E. Distinguishing between calcites formed by different mechanisms using infrared spectrometry: Archaeological applications. *J. Archaeol. Sci.* **2010**, *37*, 3022–3029. [[CrossRef](#)]
42. De La Fuente, G.A. Post-Depositional Chemical Alterations in Archaeological Ceramics: A critical review and implications for their conservation. *Boletín del Laboratorio de Petrología y Conservación Cerámica* **2008**, *1*, 21–37.
43. Hedges, R.E.M. Bone diagenesis: An overview of processes. *Archaeometry* **2002**, *44*, 319–328. [[CrossRef](#)]
44. Kendall, C.; Høier Eriksen, A.M.; Kontopoulos, I.; Collins, M.J.; Turner-Walker, G. Diagenesis of archaeological bone and tooth. *Palaeogeogr. Palaeoclimatol.* **2008**, *491*, 21–37. [[CrossRef](#)]
45. Nielsen-Marsh, C.M.; Hedges, R.E.M. Patterns of diagenesis in bone I: The effects of site environments. *J. Archaeol. Sci.* **2000**, *27*, 1139–1150. [[CrossRef](#)]

46. Rottländer, R.C.A. Über die Veränderungen von Elementkonzentrationen in keramischen Scherben während der Bodenlagerung (Teil 1). *Sprechsaal* **1981**, *114*, 742–745.
47. Aoyama, H.; Yamagiwa, K.; Fujimoto, S.; Izumi, J.; Ganeko, S.; Kameshima, S. Non-destructive elemental analysis of prehistoric potsherds in the southern Ryukyu Islands, Japan: Consideration of the pottery surface processing technique in the boundary region between the Japanese Jōmon and Neolithic Taiwan. *J. Archaeol. Sci. Rep.* **2020**, *33*, 102512. [[CrossRef](#)]
48. Snoeck, C.; Lee-Thorp, J.A.; Schulting, R.J. From bone to ash: Compositional and structural changes in burned modern and archaeological bone. *Palaeogeogr. Palaeoclimatol.* **2014**, *416*, 55–68. [[CrossRef](#)]
49. Snoeck, C.; Lee-Thorp, J.; Schulting, R.; de Jong, J.; Debouge, W.; Mattielli, N. Calcined bone provides a reliable substrate for strontium isotope ratios as shown by an enrichment experiment. *Rapid Commun. Mass Spectrom.* **2015**, *29*, 107–114. [[CrossRef](#)]
50. Snoeck, C.; Staff, R.A.; Brock, F. A reassessment of the routine pretreatment protocol for radiocarbon dating cremated bones. *Radiocarbon* **2016**, *58*, 1–8. [[CrossRef](#)]
51. Quarato, E.; Giblin, J.I. Burning Questions about Preservation: An Investigation of Cremated Bone Crystallinity at a Bronze Age Cemetery. Poster Presented at the 82nd Annual Meeting of the Society for American Archaeology, Vancouver, CO, Canada, 29 March–2 April 2017.
52. Salminen, R.; Batista, M.J.; Bidovec, M.; Demetriades, A.; De Vivo, B.; De Vos, W.; Duris, M.; Gilucis, A.; Gregorauskiene, V.; Halamic, J.; et al. *FOREGS Geochemical Atlas of Europe*; Geological Survey of Finland: Espoo, Finland, 2005.
53. Salisbury, R.B. Sediments, Settlements, and Space: A practice approach to Late Neolithic communities on the Great Hungarian Plain. Ph.D. Thesis, State University of New York at Buffalo, Buffalo, NY, USA, 2010.
54. Giblin, J.I.; Knudson, K.J.; Bereczki, Z.; Pálfi, G.; Pap, I. Strontium isotope analysis and human mobility during the Neolithic and Copper Age: A case study from the Great Hungarian Plain. *J. Archaeol. Sci.* **2013**, *40*, 227–239. [[CrossRef](#)]